

Studies of Surface Wettability Conversion on TiO<sub>2</sub> Single-Crystal Surfaces

Rong Wang,<sup>†,§</sup> Nobuyuki Sakai,<sup>†</sup> Akira Fujishima,<sup>†,\*</sup> Toshiya Watanabe,<sup>‡</sup> and Kazuhito Hashimoto<sup>‡</sup>

Department of Applied Chemistry, Faculty of Engineering, University of Tokyo, 7-3-1 Hongo, Bunkyo-ku, Tokyo 113-8656, Japan, and Research Center for Advanced Science and Technology, University of Tokyo, 4-6-1 Komaba, Meguro-ku, Tokyo 153-8904, Japan

Received: August 18, 1998; In Final Form: January 14, 1999

Reversible surface wettability conversion on titanium dioxide (TiO<sub>2</sub>) single crystals has been achieved, and its mechanism has been examined by means of contact angle measurement and X-ray photoelectron spectroscopy (XPS). A UV light illuminated TiO<sub>2</sub> single-crystal surface exhibited a 0° contact angle for both water and oil, indicative of a highly amphiphilic surface against its native hydrophobic surface. This was ascribed to photoreduction of surface Ti<sup>4+</sup> to Ti<sup>3+</sup> at definite sites, leading to preferential adsorption of dissociative water on top. A long-term storage of the highly amphiphilic surface resulted in reconversion of the surface wettability. It was found that the amphiphilic-to-hydrophobic reconversion is due to the replacement of the adsorbed hydroxyl groups by oxygen, which returns the surface geometric and electronic structures similar to the native TiO<sub>2</sub> surface. The result of angle-resolved XPS measurement revealed that the surface reactions occurred at the uppermost layers of the single crystals. By comparing the reactivities of (110), (100), and (001) single-crystal surfaces, it was concluded that oxygen bridging sites played an important role in the surface wettability conversions.

## Introduction

The rapid development of surface science and technology has remarkably facilitated progress in understanding the physical and chemical properties of semiconductor surfaces. Among the various semiconductor materials, titanium dioxide (TiO<sub>2</sub>) has attracted extensive interest due to its potential usage in industry.<sup>1–3</sup> As a typical semiconductor, excitation of TiO<sub>2</sub> with photon energy higher than its band gap gives rise to excited-state electrons and holes at conduction band and valence band, respectively, which can initiate various redox reactions at the semiconductor surface or interface. The strong oxidizing power of the photogenerated holes, the chemical inertness, and the nontoxicity of TiO<sub>2</sub> have made it a superior photocatalyst.<sup>4,5</sup> From the discovery of photoinduced water splitting on TiO<sub>2</sub> electrodes in 1972,<sup>6</sup> research has been done on enhancing the photocatalytic efficiency, mainly related to energy renewal and energy storage.<sup>7–11</sup> In recent years, applications to environmental cleanup have been one of the most active topics in photocatalysis. We have achieved purification of polluted water and air by using the strong oxidizing power of TiO<sub>2</sub> under intense UV-light illumination.<sup>12</sup> On the other hand, highly efficient TiO<sub>2</sub> thin films, coated on various substrates, have been used to decompose very small amount of pollutants in living spaces under very weak UV light lighting such as fluorescent light.<sup>13,14</sup>

The industrial demand of TiO<sub>2</sub> in photocatalysis has inspired research on surface structure of this material. Surface defects and surface-adsorbed species have been known to significantly

influence the electronic structure and the geometric structure of TiO<sub>2</sub> surface,<sup>5,15–17</sup> and in turn alter its chemical reactivity.<sup>18–20</sup> This has resulted in increasing interest in understanding and characterizing the surfaces at the microscopic level, which helps reveal the relation between surface structure and chemical reactivity. In this research field, most work has concentrated on working out the reactive sites for the gas–solid or liquid–solid interfacial reactions.<sup>18–20</sup> However, little attention has been paid to the light-induced conversion of physical and chemical characteristics of the surface itself. We have recently found that UV illumination of TiO<sub>2</sub> could create a surface that allows both water and oil to spread extensively on the common ground.<sup>21</sup> Investigations by friction-force microscopy and Fourier transform infrared spectroscopy indicated that generation of the amphiphilic surface is ascribed to the alternating distribution of hydrophilic and oleophilic regions, at the scale of several tens of nanometers, that are induced by UV illumination.<sup>22</sup> The unique amphiphilic surface character has been achieved on both single crystals and polycrystalline thin films coated on various substrates, e.g., glass, ceramics, plastics, metals, and polymer films. It has been widely expected that the laboratory results can be converted to practical products due to its antifogging and self-cleaning effects.<sup>21,22</sup>

Since the light-induced amphiphilic surface can be reversed to a hydrophobic one when it is stored in the dark for a period of time, it is necessary to clarify the mechanism so that the reverse process can be effectively prevented. In the present work, we have extensively investigated the surface reactions pertaining to the reversible surface wettability conversions. Single crystals, which provide the control over surface structures, were used in this study. On the basis of results from X-ray photoelectron spectroscopy (XPS) as well as contact angle measurements, the mechanism of the surface reactions has been analyzed. In

\* Author to whom correspondence should be addressed.

<sup>†</sup> Department of Applied Chemistry, Faculty of Engineering, University of Tokyo.

<sup>‡</sup> Research Center for Advanced Science and Technology, University of Tokyo.

<sup>§</sup> Present address: Chemical Science and Technology Division, Los Alamos National Laboratory, Los Alamos, NM 87545.

**TABLE 1: Contact Angles<sup>a</sup> of HOPG<sup>b</sup> and TiO<sub>2</sub>(110) Single Crystals with Different Liquid Species**

solid sample	liquid species			
	water	ethylene glycol	tetralin	hexadecane
HOPG	75	66	0	3
TiO <sub>2</sub> (bef. UV) <sup>c</sup>	74	44	12	7
TiO <sub>2</sub> (aft. UV) <sup>c</sup>	0	0	0	0

<sup>a</sup> Unit for contact angle is "degree". <sup>b</sup> Freshly cleaved (0001) surface of highly oriented pyrolytic graphite. <sup>c</sup> "bef. UV" stands for before UV illumination; "aft. UV" means after UV illumination. UV illumination is of 40 mW/cm<sup>2</sup> for 30 min.

addition, the distinct reactivities on different crystal faces have been discussed.

## Experimental Section

10 × 10 × 1 mm<sup>3</sup> TiO<sub>2</sub>(110), (100), and (001) single crystals from Nakazumi Crystal Laboratory were used in this study. The commercial single crystals had been well-pretreated, which was confirmed by the clear Ti 2p core level XPS signals that contains only a simple spin-orbit doublet, indicative of the lack of titanium at low oxidation states. The limited C 1s signal demonstrated that the surfaces were scarcely contaminated. However, prior to the experiments of contact angle measurements, the surfaces were further cleaned by pure acetone and Millipore-purified water. The single crystals for XPS measurements were cleaned by Ar<sup>+</sup> bombardment (E = 3000 eV) in UHV for 5 min, and subsequently annealed at 873 K in O<sub>2</sub> for 30 min. The XPS spectra demonstrated that such surfaces were nearly defect free and completely clean.

XPS spectra were acquired in an ultrahigh vacuum system with a Perkin-Elmer 5600 X-ray photoelectron spectrometer, which was equipped with a support assembly for Ar<sup>+</sup> sputtering and a separate chamber for heating in O<sub>2</sub> gas. Mg Kα X-rays were used to generate the spectra. The spectra were generally collected at a takeoff angle of 45° with respect to the surfaces of the crystals except for the angle-resolved measurements as specified in the text. The multiplex data were collected with a pass energy of 58.7 eV. The base pressure of the UHV system was at the level of 10<sup>-10</sup> Pa, and the base pressure in the pre-vacuum chamber was 10<sup>-7</sup> – 10<sup>-8</sup> Pa. UV illumination was carried out through a silica window by setting the sample in the pre-vacuum chamber.

Contact angle measurements were performed under room temperature (~295 K) using a commercial contact angle meter (FACE, Japan), with an experimental error of ±1°. UV illumination was carried out using a Hg–Xe lamp with an optical fiber coupler, employing a filter to obtain light with a wavelength centered at 365 nm.

## Results and Discussion

**Achievement of Highly Amphiphilic Surfaces.** We typically used TiO<sub>2</sub>(110) single crystals for this study. Liquids with various surface tensions were employed for contact angle measurements. A freshly cleaved surface of highly oriented pyrolytic graphite (HOPG), a conventional hydrophobic surface, was selected as a reference. As listed in Table 1, HOPG shows high contact angles with watery liquids (e.g., water and ethylene glycol), and low contact angles with oily liquids (e.g., tetralin and hexadecane), which illustrates that HOPG surface is hydrophobic and oleophilic. This agrees with the conventional concept on wetting: the hydrophobicity of a surface results from the uniform distribution of hydrophobic groups that provide relatively low adhesion tension to watery liquids but relatively

high adhesion tension to oily liquids. A TiO<sub>2</sub> single crystal prior to UV illumination shows similar surface wettability to that of HOPG, indicating a hydrophobic and oleophilic surface. However after the same surface is exposed to UV light of 40 mW/cm<sup>2</sup> for 30 min, all four liquids exhibit a contact angle of 0° ± 1° on it. This can be seen in a straightforward manner in the pictures in Figure 1, where the sequences of spreading of both water and hexadecane on a UV-illuminated TiO<sub>2</sub> surface have been demonstrated. The shape differences between a water droplet and a hexadecane droplet are due to the usage of Teflon tips that are hydrophobic and oleophilic. The observation yields the conclusion that the light-stimulated TiO<sub>2</sub> surface has equivalent affinity for both water and oil. It was found that water spread faster than hexadecane, presumably due to the difference in their viscosities. As discussed in our previous papers,<sup>21,22</sup> the formation of the amphiphilic surface is ascribed to the light-produced hydrophilic domains on an originally hydrophobic surface, leading to microstructured composition of hydrophilic and oleophilic phases on the common ground, hence both water and oil can spread extensively on it, resembling a two-dimensional capillary phenomenon.

Photogeneration of the amphiphilic surface depends on the time of UV illumination. As illustrated in Figure 2, both water contact angle and hexadecane contact angle decrease with illumination time. Our results of time-resolved friction force microscopic measurements showed that the size of hydrophilic domains grew with UV illumination time. This allows for the tentative consideration that the growth of the hydrophilic domains increases the hydrophilicity of the surface, whereas the decrease of the dimension of the oleophilic area enhances the capillary attraction, thereby facilitating the spreading of oil. As the hydrophilic/oleophilic domain sizes reach critical values, extensive spreading of both water and oil can be achieved on the same surface. It is expected that when the hydrophilic domain size becomes larger than the critical value, in other words, the oleophilic domain size becomes smaller, the surface wettability will be reversed. Our preliminary data have confirmed that the surface does become relatively hydrophilic and oleophobic when exposed to UV light for a longer time.

The surface wettability conversion also depends on the intensity of UV light. When the light intensity was lower than 20 mW/cm<sup>2</sup>, even after a long term of UV exposure, a highly amphiphilic surface cannot be achieved. This implies that the surface wettability is governed by competitive processes as will be discussed in the subsequent text. Furthermore, when light with photon energy lower than 3.4 eV is applied to the surfaces, no high amphiphilicity can be reached. This reveals that the unique surface wettability is associated with the band-gap excitation of TiO<sub>2</sub>.

High amphiphilicity was also achieved on the (100) face, the (001) face, and even the polycrystalline thin films. The light-induced high hydrophilicity (0° contact angle with water) is always accompanied with the high oleophilicity (0° contact angle with oil) on all studied surfaces. Since the oil contact angle does not change too much upon UV illumination, in the subsequent text, we will concentrate on the discussion of water contact with various surfaces.

**Reversible Conversion of the Surface Wettability.** Experiments have been conducted under different environmental conditions: (1) ambient condition (295 K, RH 80%, in air), with relatively lower O<sub>2</sub> concentration and higher H<sub>2</sub>O concentration; (2) O<sub>2</sub> atmosphere (295 K, RH < 10%), with relatively higher O<sub>2</sub> concentration and lower H<sub>2</sub>O concentration. As shown in Figure 3a, when UV illumination of 40 mW/cm<sup>2</sup> was carried

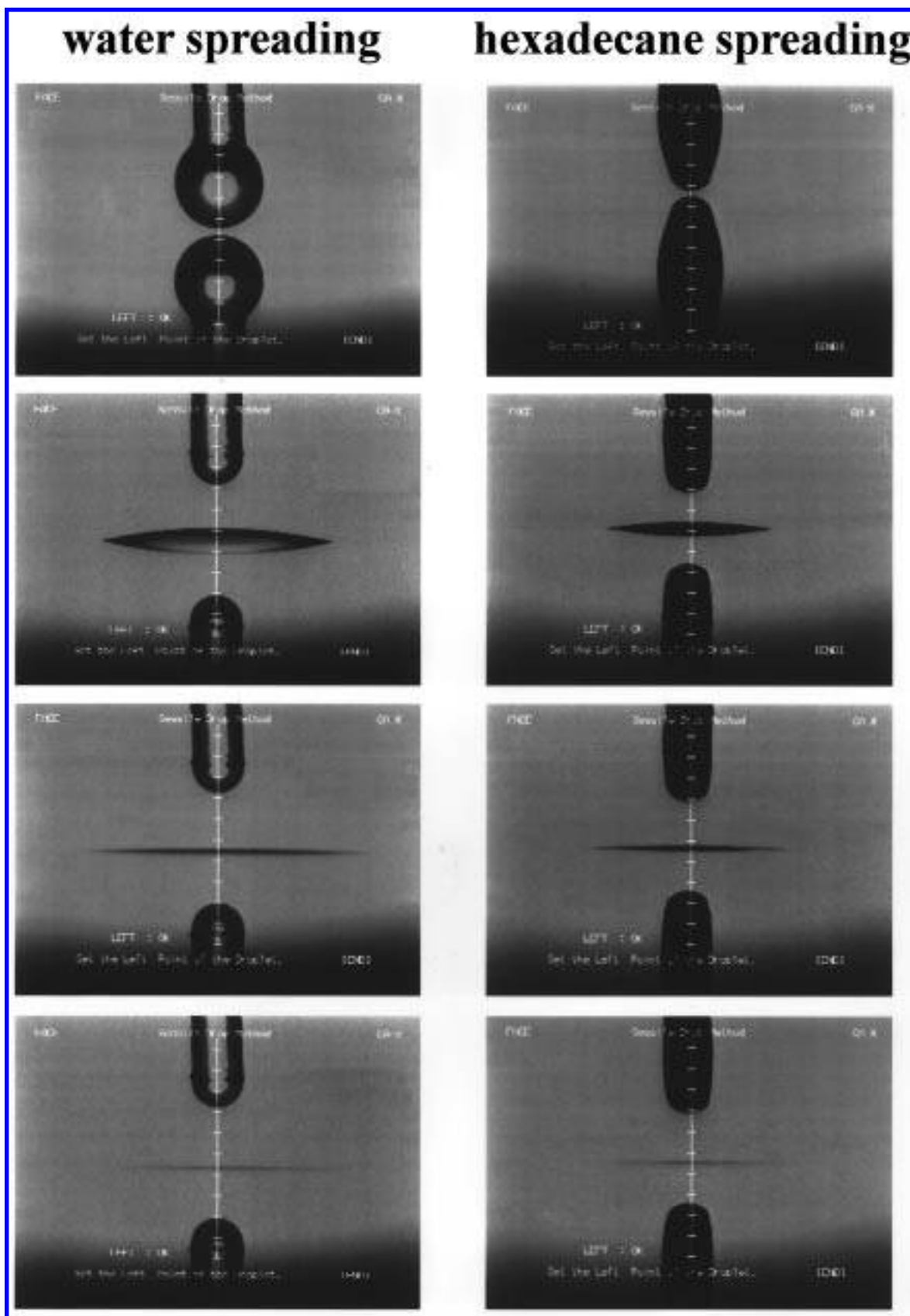


**Figure 1.** Pictures collected during contact angle measurements, showing the extensive spreadings of water and hexadecane on a UV-illuminated  $\text{TiO}_2$  (110) single-crystal surface. UV illumination:  $40 \text{ mW/cm}^2$  for 30 min under ambient condition (295 K, RH 80%, in air).

out under ambient conditions, water contact angle of the  $\text{TiO}_2$ -(110) single crystal surface quickly decreased with irradiation time (dotted line). Thirty minute illumination was sufficient to give rise to a highly hydrophilic surface. However, when UV illumination was carried out in  $\text{O}_2$  atmosphere as shown as the

solid line in Figure 3a, water contact angle of the single-crystal surface dropped at first, followed by a plateau of slow decay and eventually saturated at  $35^\circ$ . This indicates that the existence of  $\text{O}_2$  gas greatly blocked the hydrophobic-to-hydrophilic surface wettability conversion. On the other hand, when a highly

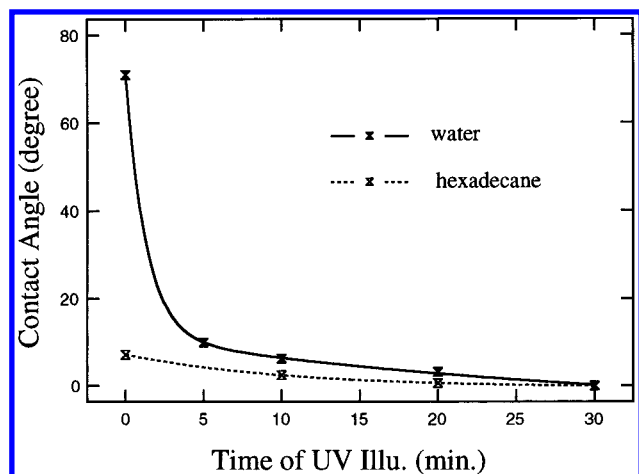


**Figure 2.** Plot of the contact angle of different liquids versus UV illumination time for a  $\text{TiO}_2(110)$  single-crystal surface. Solid line, water; dashed line, hexadecane. UV illumination: 40  $\text{mW}/\text{cm}^2$  under ambient condition (295 K, RH 80%, in air).

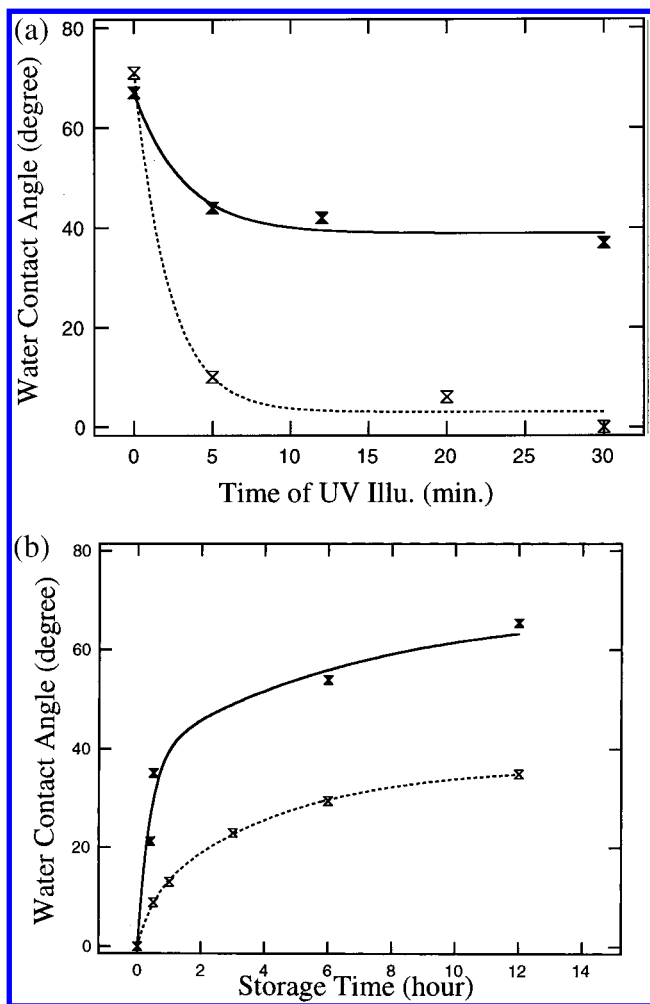


**Figure 3.** (a) Variation of the water contact angle upon UV illumination of a fresh  $\text{TiO}_2(110)$  single crystal in air (dashed line) and in an oxygen atmosphere (solid line). Light intensity: 40  $\text{mW}/\text{cm}^2$ . (b) Variation of water contact angle upon storage of a highly hydrophilic  $\text{TiO}_2(110)$  single crystal in air (dashed line) and in an oxygen atmosphere (solid line).

hydrophilic sample was stored in the dark under ambient condition, the surface gradually turned hydrophobic, as shown as the dotted line in Figure 3b. Seven days of storage of the sample in ambient condition can return its water contact angle to 70°.

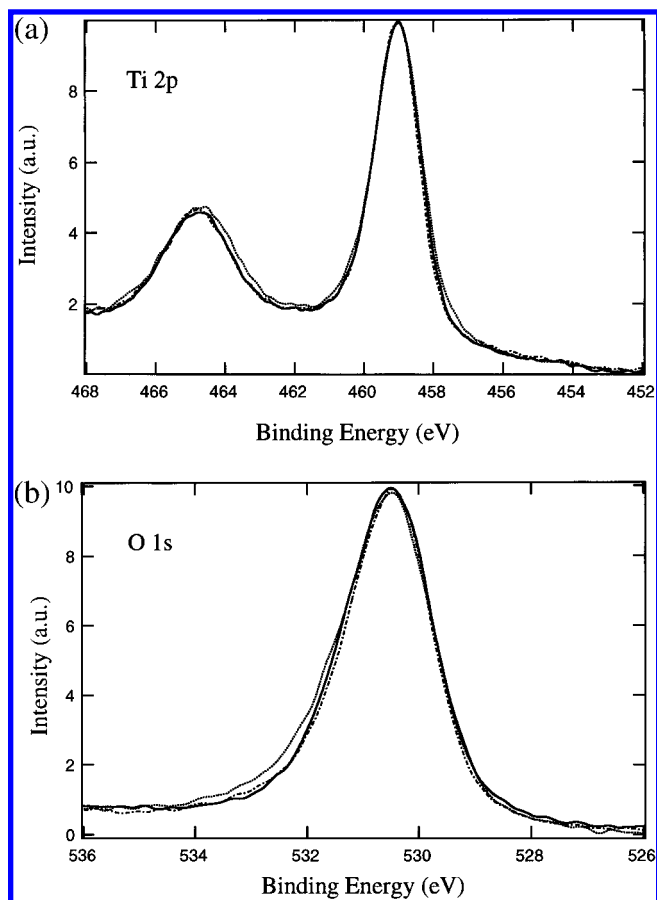


**Figure 4.** XPS spectra of Ti 2p (a) and O 1s (b) for a  $\text{TiO}_2(110)$  single-crystal surface. Solid line: nearly defect-free surface; dotted line: upon UV illumination of 30  $\text{mW}/\text{cm}^2$  for 1.5 h in  $10^{-7}$ – $10^{-8}$  Pa vacuum; broken line: upon exposure to  $\text{O}_2$  gas at 295 K for 30 min at  $\text{O}_2$  partial pressure of  $10^{-5}$  Pa.

The solid line illustrates that storage of a hydrophilic surface in  $\text{O}_2$  atmosphere remarkably facilitated the hydrophilic-to-hydrophobic reversion.

While contact angle measurement is proved to be a useful means to monitor the surface wettability change macroscopically, an XPS spectroscopic study allows the detailed investigation on the electronic structure of a surface. Figure 4 shows the variations in Ti 2p and O 1s XPS spectra of a  $\text{TiO}_2(110)$  single crystal under different conditions. The solid lines represent the spectra of a surface that was achieved by Ar ion sputtering and subsequently annealing in  $\text{O}_2$  gas as described in the Experimental Section. The symmetric shapes of both the Ti 2p band and the O 1s band demonstrate that the pretreated surface is nearly defect free. After the surface was exposed to UV light of 30  $\text{mW}/\text{cm}^2$  for 1.5 h (dotted lines) in the pre-vacuum chamber, however, the Ti 2p spectrum was slightly broadened, and a shoulder band appeared 1.6 eV lower than the  $\text{Ti}^{4+}$  binding energy, associated with the  $\text{Ti}^{3+}$  defect state.<sup>23–29</sup> Correspondingly, the O 1s band turned asymmetric with a tail at the higher binding energy side. The above observation agrees with the literature, indicating that UV illumination has generated surface defects<sup>30,31</sup> that are accompanied with electronic charge transfer from oxygen to titanium, hence the decrease of binding energy of titanium and the increase of binding energy of oxygen.<sup>29</sup> The experimental result of angle-resolved XPS spectra implies that the photogenerated defects exist at the uppermost layer of the surface. On the other hand, after the irradiated surface was stored in  $\text{O}_2$  gas at 296 K for 30 min, with a partial pressure of  $10^{-5}$  Pa, the spectra of both Ti 2p and O 1s (broken lines) became



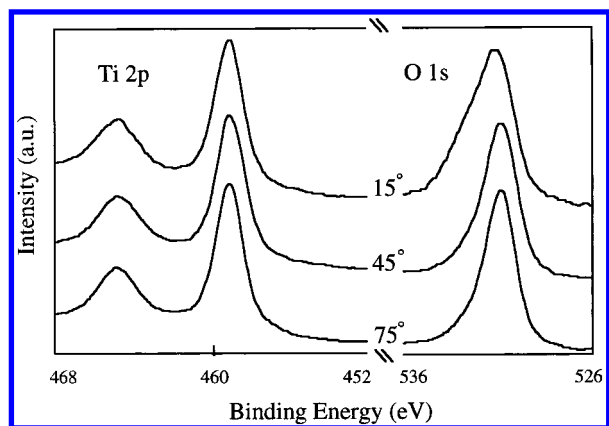


**Figure 5.** Angle resolved XPS spectra of a  $\text{TiO}_2$  (110) single-crystal surface upon UV illumination in air. UV illumination: 40  $\text{mW}/\text{cm}^2$  under ambient condition (295 K, RH 80%) for 30 min.

identical with the spectra prior to UV illumination (solid lines). These results imply that the light-induced oxygen vacancies on the top surface can be reoxidized by the adsorption of oxygen from gas phase at room temperature, which reverse both the electronic structure and the geometric structure to almost the same as the native surface.

To make XPS results comparable to that of the contact angle measurements, XPS spectra were also acquired for a (110) surface upon UV illumination in air (Figure 5). The surface was pretreated the same way as described above. The spectra were collected with photoelectrons taking off from the surface at 15°, 45°, and 75°, respectively, after the surface was exposed to UV light of 40  $\text{mW}/\text{cm}^2$  for 30 min in air (295 K, RH 80%). It was reported that the probing depth of the XPS spectra at an electron emission angle of 13° is  $\sim 4$  Å, and it is  $\sim 13$  Å at 43°. <sup>32</sup> Thereby, it is considered that the spectrum at 15° furnishes information at the uppermost layer of the single-crystal surface, and the spectrum at 75° reflects the electronic bonding in the bulk. As shown in Figure 5, the Ti 2p spectrum scarcely changes with the electron emission angle, whereas significant differences exist among the spectra of O 1s obtained at the three angles. The O 1s spectrum acquired at 75° is analogous to the spectrum of the nearly defect-free surface (Figure 4b). With decrease of the takeoff angle, a shoulder band appears at lower energy than the O 1s band, and is maximized at the angle of 15°. This shoulder band can be fitted to two bands which are 1.5 and 2.6 eV lower than the O 1s band, corresponding to dissociative water (hydroxyl groups) adsorption <sup>28,33</sup> and molecular water adsorption, <sup>34</sup> respectively. The lack of change of the Ti 2p band is due to healing of the light-induced surface  $\text{Ti}^{3+}$  defects by adsorption species, e.g., oxygen and water. Unfortunately, XPS is not able to distinguish among a defect-free surface, an oxygen-healed defective surface, and a hydroxyl-healed defective surface at the Ti 2p region. <sup>26,28</sup> However, considering the change of the O 1s band, the results of Figure 5 suggest that the light-induced surface defects are healed by dissociative water at the uppermost surface though adsorption of a small amount of oxygen cannot be excluded. Combining these results with our previous results from FTIR spectra and FFM images, <sup>22</sup> the adsorbed hydroxyl groups are covered by monolayer or multilayer molecular water. <sup>35</sup>

As Wang et al. reported according to their XPS results, an  $\text{OH}^-$ -healed surface is thermally less stable than an  $\text{O}_2$ -healed surface, indicating that oxygen is more strongly bonded on the defect site than is the  $\text{OH}^-$  group. <sup>28</sup> The surface with adsorbed hydroxyl species is a chemically and structurally different surface from the original  $\text{TiO}_2$  surface. It is therefore reasonable

that the adsorbed  $\text{OH}^-$  groups can be replaced by oxygen atoms, causing the reverse conversion of the surface wettability.

According to the above analysis and the previous studies, the surface reactions are conceived as follows: light with photon energy corresponding to the band gap of  $\text{TiO}_2$  photoreduces  $\text{Ti}^{4+}$  to  $\text{Ti}^{3+}$ , generating surface defects typically at oxygen bridging sites. <sup>30,31</sup> When a surface-defect site is generated in air, water and oxygen compete to dissociatively adsorb on it. The contact angle of such a surface illustrates the result of equilibrium of water adsorption and oxygen adsorption under a certain condition. As shown in Figures 3 and 5, UV illumination in air enhanced water adsorption at the defect sites on the topmost surface. This indicates that the defect sites are more favorable for hydroxyl adsorption than oxygen adsorption. However, the adsorption of  $\text{OH}^-$  groups distorted the surface in both the electronic structure and the geometric structure, and the surface is energetically unstable compared with the native hydrophobic  $\text{TiO}_2$  surface. Exposing the surface to a high concentration of  $\text{O}_2$  gas breaks the adsorption balance, and the contact angle changes to follow the setup of a new adsorption balance under the current condition. As a result, oxygen adsorption becomes superior, and the surface wettability quickly reconverted from hydrophilicity to hydrophobicity. We have found that a highly amphiphilic surface can never be achieved when UV illumination is carried out in  $\text{O}_2$  gas; on the other hand, UV illumination in high humidity can more easily result in the high amphiphilicity. These observations well support the above analysis.

**Surface Reactivities on Distinct Faces.** It has been well-known that oxygen vacancies play an important role in the process of water adsorption on  $\text{TiO}_2$  single-crystal surfaces. <sup>33–37</sup> The surface defects, most likely created at bridging-O sites, act as “feeder” sites, producing dissociated species of water which diffuse to other sites where adsorption occurs. <sup>38</sup> Previous studies on friction force microscopy <sup>21,22</sup> implied that water adsorption on the  $\text{TiO}_2$ (110) surface is associated with the alignment of oxygen bridging sites. Due to the distinct surface structures of different faces, it is expected that the behaviors of surface wettability conversion should be different on individual single-crystal planes.

Figure 6, parts a and b, show the results of water contact angle measurements following UV illumination applied to a (100) face and (001) face, respectively. Comparing this with Figure 3a, the process of hydrophobic to hydrophilic conversion on (100) face is similar to that of (110) face, i.e., the water contact angle quickly decreased with the time of UV illumination in air; however, the water contact angle decreased and saturated at 38° when UV light was applied to the surface in  $\text{O}_2$  atmosphere. The (001) face shows completely different wetting behavior from both the (110) face and the (100) face. The surface is inert when it exposed to UV light in air for a short time. With a longer time exposure, the surface gradually turned hydrophilic. The (001) face is unconvertible in high concentration of  $\text{O}_2$  gas, even under a long period of UV exposure.

Correspondingly, surface defects on (110), (100), and (001) faces were also examined by XPS measurements in a vacuum. Similar to the spectra in Figure 4, a shoulder band at lower binding energy, associated with  $\text{Ti}^{3+}$  states, appeared in the Ti 2p spectra of both the (100) face and the (001) face when UV light was applied to them. The intensity ratio between the  $\text{Ti}^{3+}$  band and the  $\text{Ti}^{4+}$  band can be evaluated, allowing for the quantitative calculation of the surface defect sites (see Supporting Information). The results of such calculations for (110),

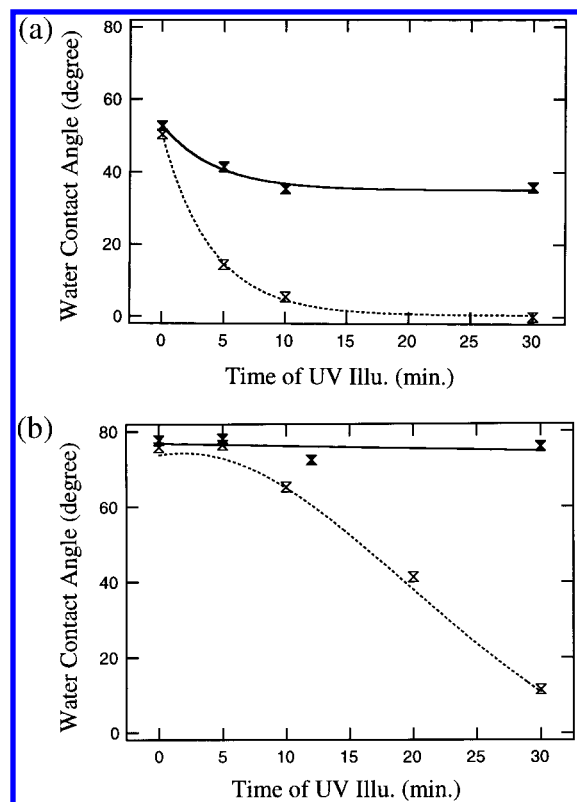


**Figure 6.** Variations of the water contact angle upon UV illumination of (a), (100) face; (b), (001) face. Dashed line, in air; solid line, in oxygen atmosphere. Light intensity: 40 mW/cm<sup>2</sup>.

(100), and (001) faces indicate that defects can be relatively easily produced on (110) and (100) faces, whereas the (001) face exhibits a relatively inert surface. With the results of water contact angle measurements in Figure 6, it suggests that surface wettability conversion greatly depends on the amount of light-induced defect sites that are relevant to the surface structure of the TiO<sub>2</sub> single crystal.

The different conversion behaviors among the various single crystal faces can be rationalized by comparing their surface atom alignments as shown in Figure 7. One-half of the Ti cations on a perfect (110) surface are 5-fold coordinated, with the remaining one-half being 6-fold coordinated as in the bulk. The (100) surface has only 5-fold coordinated surface Ti cations, while the (001) surface has all its Ti cations only 4-fold coordinated.<sup>39,40</sup> The electronic structures of the (110) and the (100) surfaces are similar in that the 5-fold coordinated Ti ions on both surfaces have the same O ligand environment. Furthermore, bridging site oxygens, which are higher in position and energetically more reactive than their surrounding atoms, exist on both of the planes. The slight difference between them is that the oxygen anions on the (100) surface are rotated by 45° relative to those on the (110) surface, and thus the perfect (100) surface is more active to dissociative water adsorption than an ideal (110) surface.<sup>36</sup> This is supported by the results of contact angle measurements (Figures 3a and 6a) in that an initial (100) surface showed a water contact angle of 55° against the 72° of an initial (110) surface. On the other hand, the (001) surface differs from the (110) and (100) surfaces in that all the surface Ti cations are 4-fold coordinated with two oxygen within the surface plane and the other two in the plane below. The lack of bridging site oxygen on this surface leads to its inertness to UV illumination. However, calculation by Ramamoorthy et al. demonstrated that the (001) surface has the lowest surface energy among the three discussed surfaces due to the weak bonding of

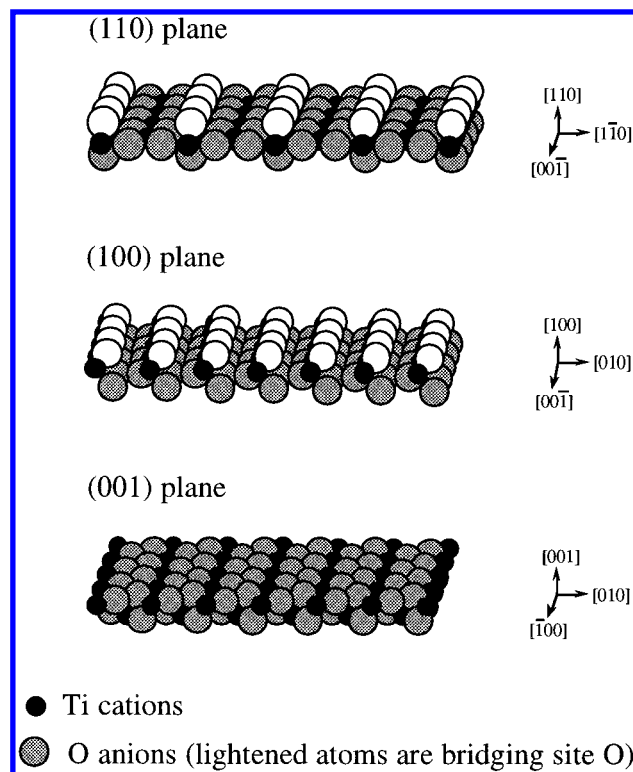


**Figure 7.** Schematic illustration of the atomic alignments on ideal TiO<sub>2</sub>(110), (100), and (001) single-crystal faces.

its surface atoms.<sup>40</sup> It is therefore plausible that a long period of UV illumination can create in-plane oxygen vacancies on the (001) face so that the gradual conversion of the surface wettability can be achieved. Accordingly, the defect sites on the (001) surface are more unstable when compared with the (110) face and the (100) face. As long as a high concentration of O<sub>2</sub> gas is supplied, the defects on the (001) plane can be totally and quickly healed even when the surface is continuously exposed to UV light, as illustrated in Figure 6b.

## Conclusions

Reversible surface wettability conversion on TiO<sub>2</sub> single-crystal surfaces has been successfully accomplished. It was found that an amphiphilic surface can be achieved by photo-reduction of Ti<sup>4+</sup> to Ti<sup>3+</sup> at definite sites on a surface, resulting in the preferential adsorption of hydroxyl groups on corresponding oxygen vacant sites. The reconversion of an amphiphilic surface to a hydrophobic surface was also obtained upon storage in the dark. This was attributed to the replacement of the adsorbed hydroxyl groups by oxygen in air, which has been confirmed by the results of XPS measurements. A further evidence to support the mechanism described here comes from the fact that ultrasonic irradiation of an amphiphilic surface in pure water greatly facilitated the amphiphilic to hydrophobic reconversion process, due to the creation of OH radicals which possess strong oxidizing power and thus accelerate the reconversion.<sup>41</sup> Another interesting finding of the present study is that different faces of TiO<sub>2</sub> single crystals displayed distinct wetting behaviors, which will serve as the guideline to select proper surfaces for practical applications, e.g., antifogging and self-cleaning.

Practically, instead of single crystals, polycrystalline TiO<sub>2</sub> films are widely used due to their lower cost and ease of coating on various materials. Accordingly, extensive work has also been performed on polycrystalline anatase films. It was found that

an amphiphilic surface was more easily achieved on polycrystalline anatase films with light intensity as low as 0.1 mW/cm<sup>2</sup> and a much shorter time of UV illumination. Such results can be ascribed to either the type of titanium dioxide (rutile or anatase) or the polycrystallinity. Related work is being done to look into the details.

After all, the surface wettability conversion and reconversion are due to the formation and removal of the nanoscale domain structures.<sup>21,22</sup> The unique amphiphilic surface property is a result of the characteristic microstructure. It is therefore important to explore alternative methods to create amphiphilic surfaces. Our recent investigation has revealed that surface treatments of TiO<sub>2</sub> via Ar<sup>+</sup> sputtering and annealing can also give rise to amphiphilic surfaces.<sup>42</sup> These results allow us to further infer that the amphiphilic surface property generally exists on a surface of any material that is composed of alternately distributed hydrophilic and oleophilic domains at a scale lower than the critical size. Referring to the amphiphilic surface property as a typical example, the macroscopic physical or chemical characteristics of a material should be closely related to its microscopic structure; one could go further and say that when the microscopic structure of a material can be controllably regulated, achievement of desired macroscopic properties can be anticipated.

**Acknowledgment.** R.W. acknowledges the financial support of the Japan Society for the Promotion of Science (JSPS).

**Supporting Information Available:** Calculation of ratios of surface defects on (110), (100), and (001) faces, generated by UV illumination. This material is available free of charge via the Internet at <http://pubs.acs.org>.

## References and Notes

- (1) Heller, A. *Acc. Chem. Res.* **1995**, 28, 503.
- (2) (a) Fujishima, A. Proceedings of the 11th International Conference on Photochemical Conversion and Storage of Solar Energy; 1996. (b) Fujishima, A.; Hashimoto, K.; Watanabe, T. In *Light Cleaning Revolution*, (in Japanese). English version is in preparation.
- (3) Hoffmann, M. R.; Martin, S. T.; Choi, W.; Bahnemann, D. W. *Chem. Rev.* **1995**, 95, 69.
- (4) Fox, M. A.; Dulay, M. T. *Chem. Rev.* **1993**, 93, 341.
- (5) Linsebigler, A. L.; Lu, G.; Yates, J. T., Jr. *Chem. Rev.* **1995**, 95, 735.
- (6) Fujishima, A.; Honda, K. *Nature* **1972**, 238, 37.
- (7) Chang, K. C.; Heller, A.; Schwartz, B.; Menezes, S.; Miller, B. *Science* **1977**, 196, 1097.
- (8) Tufts, B. J.; Abrahams, I. L.; Santangelo, P. G.; Ryba, G. N.; Casagrande, L. G.; Lewis, N. S. *Nature* **1987**, 326, 861.
- (9) Licht, S.; Peramunage, D. *Nature* **1990**, 345, 330.
- (10) O'Regan, B.; Grätzel, M. *Nature* **1991**, 353, 737.
- (11) Kawai, T.; Sakata, T. *Nature* **1980**, 286, 474.
- (12) Takawa, Y.; Hashimoto, K.; Fujishima, A. In preparation.
- (13) (a) Ohko, Y.; Hashimoto, K.; Fujishima, A. *J. Phys. Chem. A* **1997**, 101, 8057. (b) Sopyan, I.; Watanabe, M.; Murasawa, S.; Hashimoto, K.; Fujishima, A. *J. Photochem. Photobiol. A: Chem.* **1996**, 98, 79.
- (14) Sunada, K.; Kikuchi, Y.; Hashimoto, K.; Fujishima, A. *Environ. Sci. Technol.* **1998**, 32, 726.
- (15) Chen, J. G. *Surf. Sci. Rep.* **1997**, 30, 1.
- (16) Murray, P. W.; Condon, N. G.; Thornton, G. *Surf. Sci. Lett.* **1995**, 323, L281.
- (17) Rohrer, G. S.; Henrich, V. E.; Bonnell, D. A. *Science* **1990**, 250, 1239.
- (18) Rusu, C. N.; Yates, J. T., Jr. *Langmuir* **1997**, 13, 4311.
- (19) Lu, G.; Linsebigler, A.; Yates, J. T., Jr. *J. Phys. Chem.* **1994**, 98, 11733.
- (20) Engel, T. *Langmuir* **1996**, 12, 1428.
- (21) Wang, R.; Hashimoto, K.; Fujishima, A.; Chikuni, M.; Kojima, E.; Kitamura, A.; Shimohigoshi, M.; Watanabe, T. *Nature* **1997**, 388, 431.
- (22) Wang, R.; Hashimoto, K.; Fujishima, A.; Chikuni, M.; Kojima, E.; Kitamura, A.; Shimohigoshi, M.; Watanabe, T. *Adv. Mater.* **1998**, 10, 135.
- (23) Eriksen, S.; Egdell, R. G. *Surf. Sci.* **1987**, 180, 263.
- (24) Idriss, H.; Barteau, M. A. *Catal. Lett.* **1994**, 26, 123.
- (25) Sanjinés, R.; Tang, H.; Berger, H.; Gozzio, F.; Margaritondo, G.; Lévy, F. J. *Appl. Phys.* **1994**, 75, 2945.
- (26) Shultz, A. N.; Jang, W.; Hetherington, W. M., III; Baer, D. R.; Wang, L. Q.; Engelhard, M. H. *Surf. Sci.* **1995**, 339, 114.
- (27) Pan, J. M.; Maschhoff, B. L.; Diebold, U.; Madey, T. E. *J. Vac. Sci. Technol. A* **1992**, 10, 2470.
- (28) Wang, L. Q.; Baer, D. R.; Engelhard, M. H.; Shultz, A. N. *Surf. Sci.* **1995**, 344, 237.
- (29) Göpel, W.; Anderson, J. A.; Frankel, D.; Jaehnic, M.; Phillips, K.; Schäfer, J. A.; Rucker, G. *Surf. Sci.* **1984**, 139, 333.
- (30) Highfield, J. G.; Grätzel, M. *J. Phys. Chem.* **1988**, 92, 464.
- (31) Lo, W. J.; Chung, Y. W.; Somorjai, G. A. *Surf. Sci.* **1978**, 71, 199.
- (32) Wandelt, K. *Surf. Sci. Rep.* **1985**, 2, 1.
- (33) Thiel, P. A.; Madey, T. E. *Surf. Sci. Rep.* **1987**, 7, 211.
- (34) Hugenschmidt, M. B.; Gamble, L.; Campbell, C. T. *Surf. Sci.* **1994**, 302, 329.
- (35) Traversa, E. *Sens. Actuators, B* **1995**, 23, 135.
- (36) Henderson, M. A. *Langmuir* **1996**, 12, 5093.
- (37) Henderson, M. A. *Surf. Sci.* **1996**, 355, 151.
- (38) Kurtz, R. L.; Stockbauer, R.; Madey, T. E.; Román, E.; De Segovia, J. L. *Surf. Sci.* **1989**, 218, 178.
- (39) Henrich, V. E.; Kurtz, R. L. *Phys. Rev. B* **1981**, 23, 6280.
- (40) Ramamoorthy, M.; Vanderbilt, D.; King-Smith, R. D. *Phys. Rev. B* **1994**, 49, 16721.
- (41) Sakai, N.; Wang, R.; Fujishima, A.; Watanabe, T.; Hashimoto, K. *Langmuir* **1998**, 14, 5918.
- (42) Wang, R.; Jiang, L.; Sawunyama, P.; Hashimoto, K.; Fujishima, A. In preparation.